Modeling the effect of tilting, passive leg exercise, and functional electrical stimulation on the human cardiovascular system

Med Biol Eng Comput (2017) 55:1693–1708
DOI 10.1007/s11517-017-1628-8

ORIGINAL ARTICLE

Modeling the effect of tilting, passive leg exercise, and functional electrical stimulation on the human cardiovascular system

Amirehsan Sarabadani Tafreshi[1,2] · **Jan Okle**[1] · **Verena Klamroth-Marganska**[1,2] · **Robert Riener**[1,2]

Received: 6 October 2016 / Accepted: 27 January 2017 / Published online: 10 February 2017

Abstract Long periods of bed rest negatively affect the human body organs, notably the cardiovascular system. To avert these negative effects and promote functional recovery in patients dealing with prolonged bed rest, the goal is to mobilize them as early as possible while controlling and stabilizing their cardiovascular system. A robotic tilt table allows early mobilization by modulating body inclination, automated passive leg exercise, and the intensity of functional electrical stimulation applied to leg muscles (inputs). These inputs are used to control the cardiovascular variables heart rate (HR), and systolic and diastolic blood pressures (sBP, dBP) (outputs). To enhance the design of the closed-loop cardiovascular biofeedback controller, we investigated a subject-specific multi-input multi-output (MIMO) black-box model describing the relationship between the inputs and outputs. For identification of the linear part of the system, two popular linear model structures—the autoregressive model with exogenous input and the output error model—are examined and compared. The estimation algorithm is tested in simulation and then used in four study protocols with ten healthy participants to estimate transfer functions of HR, sBP and dBP to the inputs. The results show that only the HR transfer functions to inclination input can explain the variance in the data to a reasonable extent (on average 69.8%). As in the other input types, the responses are nonlinear; the models are either not reliable or explain only a negligible amount of the observed variance. Analysis of both, the nonlinearities and the occasionally occurring zero-crossings, is necessary before designing an appropriate MIMO controller for mobilization of bedridden patients.

Keywords Rehabilitation · Bed rest · Robotic tilt table · Closed-loop control · Biofeedback · Hammerstein model identification

1 Introduction

Severe diseases often lead to long periods of bed rest which impose serious negative consequences on the body [8, 18, 19] that can postpone the recovery and even reduce survival chances [3]. Very early mobilization can avert these negative effects, improve functional outcome and promote fast recovery in the patients [7, 9, 16, 31]. However, to enable early mobilization while avoiding any further adverse effects (e.g., fainting), patients' cardiovascular variables have to be kept within safe ranges [12].

A bed with mobilization capabilities could be suited for very early mobilization. Mobilization modules such as an integrated passive robotic exercise could be used in a closed-loop manner to control and stabilize cardiovascular variables [17]. Therefore, we aimed at designing a novel intelligent rehabilitation bed that enables automatic mobilization of bedridden patients while controlling and stabilizing their cardiovascular system [35, 36, 45]. As an initial

Electronic supplementary material The online version of this article (doi:10.1007/s11517-017-1628-8) contains supplementary material, which is available to authorized users.

✉ Amirehsan Sarabadani Tafreshi
sarabadani@hest.ethz.ch

[1] Sensory-Motor Systems (SMS) Lab, Institute of Robotics and Intelligent Systems (IRIS), Department of Health Sciences and Technology (D-HEST), ETH Zurich, Sonneggstrasse 3, 8092 Zurich, Switzerland

[2] Rehabotics Group, Spinal Cord Injury Center, Balgrist University Hospital, Medical Faculty, University of Zurich, Zurich, Switzerland

prototype, we used a robotic tilt table that allows early mobilization by adjusting body inclination and providing automated passive leg exercise (stepping) without or with application of functional electrical stimulation (FES) to leg muscles. The FES might enhance the stepping effect [10]. Therefore, these external mechanical and electrical stimuli can be considered to provide early mobilization and furthermore, as inputs to control the dynamics of cardiovascular variables, i.e., heart rate (HR), systolic and diastolic blood pressures (sBP, dBP) (see Fig. 1a).

Various control strategies were pursued before [35, 36, 45]. Initially, based on drawbacks observed in [45], where we had applied a model-based control strategy, we investigated the development of model-free control strategies [35, 36]. Still, the results advocated the need for a model-based control strategy incorporating some knowledge about the human body responses. Therefore, to enhance the controller design, in this work, we focused on the identification of models describing the cardiovascular responses to the external stimuli.

A physiological model like the one used in [45] usually possesses many parameters. The more parameters a model has, the more input variation is needed to be persistently exciting and to be able to estimate the model parameters reasonably [32]. In an identification phase before the therapy, a lot of input variation might not be possible because it can be inconvenient or even dangerous for patients. This could lead to a lack of persistency of excitation if a complex model is considered. Black-box models omit the details of internal processes and, therefore, can compress the information to describe the input-output relationship in a compact form using a few parameters. Thus, a simple low-order black-box model could be suitable for our application due to two fundamental reasons: (1) it only possesses few parameters, and therefore, little input variation is needed for its identification; (2) it can be identified in a patient-specific way and independently from the underlying disease. Such a simplified model could also be consistent with the goal of our closed-loop multi-input multi-output (MIMO) biofeedback controller to control the long-term dynamics (i.e., mean changes) of cardiovascular variables rather than detailed changes. Therefore, in this work, we considered identification of low-order (i.e., first- or second-order) models. This decision was also supported by other works focusing on the development of cardiovascular biofeedback systems to control long-term dynamics of cardiovascular variables. Most of these works have also usually considered low-order models (e.g., first-order model in [42] or second-order model in [14]) and even the works which have considered higher orders, have usually found that a first-order model is sufficient to capture the system dynamics (e.g.,

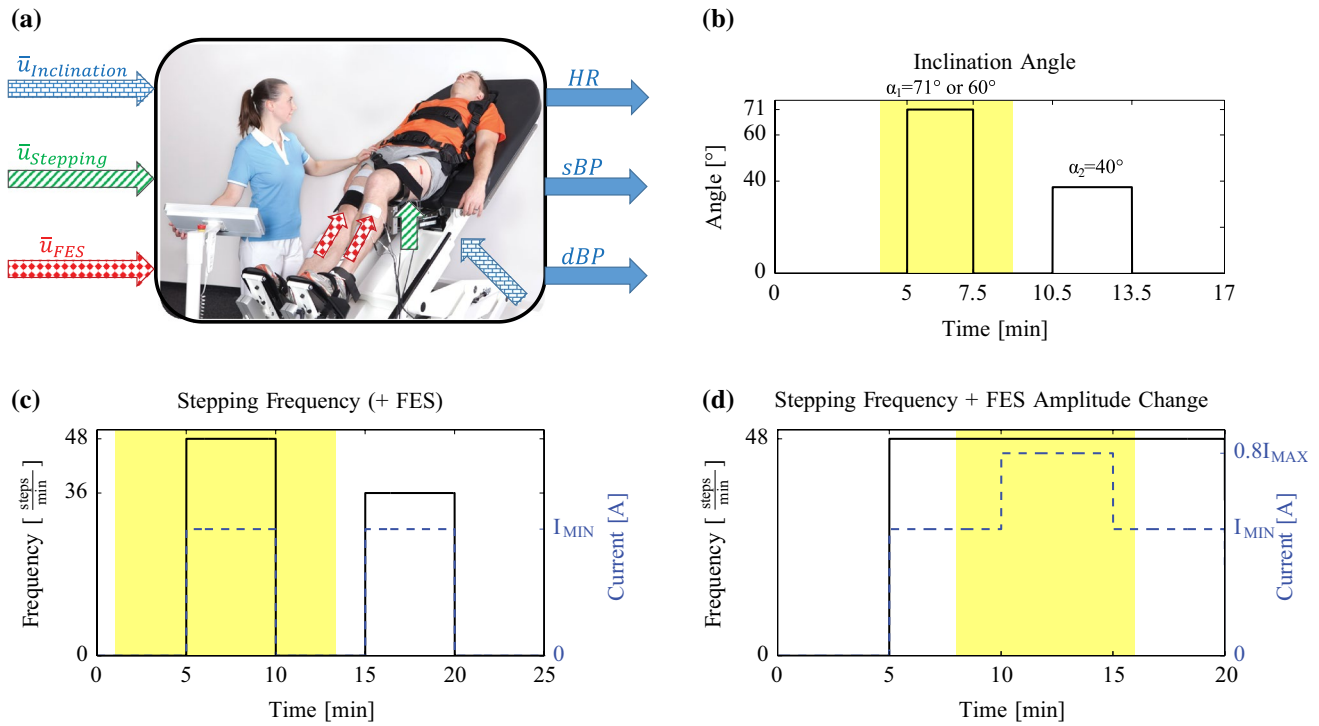

Fig. 1 **a** Diagram of inputs and outputs of the system (Picture adapted with permission from Hocoma AG, Switzerland.). **b** Study Protocol 1: Change of inclination angle in two experiments ($\alpha = 71°$ experiment, $\alpha = 60°$ not shown). **c** Study Protocols 2 and 3: Change of Stepping Frequency (*solid*) without and with application of minimum FES amplitude (*dashed*). **d** Study Protocol 4: Change of FES amplitude (*dashed*) during constant stepping (*solid*). The *highlighted areas* show the data range used for model identification

[13]). Having a simple model, issues such as nonlinearities, time-variance, etc. could still be addressed in the controller design using standard methods.

The contributions of the current work are twofold: First, we present a systematic approach to estimate low-order models of the human cardiovascular system response using black-box identification. The method uses *K*-fold cross-validation technique [6] that enables efficient use of limited data for model estimation. For the identification of the linear part, we discuss two popular linear model structures; the AutoRegressive model with eXogenous input (ARX) and Output Error model (OE) [27]. To consider nonlinearity in the models, the Hammerstein model structure [2] which is widely used for nonlinear modeling of physiological processes (e.g., in [24]) is considered and advantages of applying a step input over other input types such as pseudorandom binary sequence (PRBS) or frequency sweep, when two-step (independent linear and nonlinear part) identification of such systems [2] for development of biofeedback systems is desired, is discussed.

Second, the estimation algorithm is tested in simulation and then applied in four study protocols (see Fig. 1b–d) with ten healthy participants to estimate the transfer functions (TFs) of the cardiovascular responses (HR, sBP and dBP) to (1) passive tilting, (2) passive leg exercise (stepping) without and (3) with FES of leg muscles, and (4) modulation of FES intensity applied to the leg muscles, while rejecting the cardiovascular natural oscillations as noise. Based on the identified individual-specific MIMO systems from the experiments, we discuss potential challenges in the development of the cardiovascular biofeedback system for very early mobilization of bed-rest patients from a control engineering perspective. Furthermore, based on the simulation and experimental results, we compare the performance of the ARX and OE structures for identification of first- and second-order models in the context of cardiovascular biofeedback systems.

2 Materials and methods

2.1 Robotic tilt table and measurement equipment

The Erigo (Hocoma AG, Switzerland) is a robotic rehabilitation tilt table designed for early mobilization of bed-rest patients and allows simultaneous verticalization and automated stepping training [11]. The inclination angle α of the table can be continuously adjusted between 0° and 75°, where the effective maximum in our experiments was measured to be 71°. The motor-driven stepping module can automatically move the subject's legs in a passive manner with equal extension and flexion periods and adjustable speeds between 0 and 80 steps per minute. The stepping consists of passive leg movements and cyclic leg loadings produced by two springs beneath the subject's feet. It is believed that the stepping can enhance muscle pump function and venous return, and therefore, improve cardiovascular stability [28]. The table is furthermore equipped with an FES module that can stimulate the muscles of the legs during the passive stepping. The robotic tilt table also has a harness to fix the subject and minimize the weight bearing during the therapy.

The raw blood pressure (BP) signal was measured using a CNAP® monitor 500 (CNSystems Medizintechnik AG, Austria). The monitor uses a finger cuff and an arm cuff to measure the BP signal. Before starting each measurement, it needs a short calibration phase (about 2 min). The BP measurement was done on the right arm of the subjects. For an accurate measurement, a sling was used to keep the arm and hand relaxed at the heart level.

To compute the biosignals (i.e., HR, sBP, and dBP), the raw BP signal (analog) was read out at 100 Hz from the monitor and sent to the tilt table PC. The signal was buffered online, and its maxima (sBP) and minima (dBP) values were detected. The HR values were computed using the heart period calculated based on the time interval between consecutive dBP values. The beat-to-beat values of HR, sBP, and dBP were then linearly interpolated at about 3.3 Hz (sampling time 0.3 s). For data processing, the input stimuli signals (e.g., 48 steps per minute constant signal of stepping) were also discretized at the same frequency.

2.2 Participants

Ten healthy male subjects participated in the study (see Table 1). The subjects had no known cardiovascular disease and were not taking any medication. They were

Table 1 Participants' data

Participant	Age (year)	Weight (kg)	Height (cm)	BMI[a]
1	28	86.8	168	30.8
2	28	72.0	182	21.7
3	22	91.4	182	27.6
4	23	85.1	179	26.6
5	24	70.4	182	21.3
6	30	78.6	184	23.2
7	24	75.5	174	24.9
8	24	89.6	195	23.6
9	25	79.8	183	23.8
10	23	81.2	183	24.2
Mean	25.1	81.0	181.2	24.8
SD	2.6	7.2	6.97	2.9

[a] Body mass index

instructed not to consume caffeine, alcohol or nicotine eight hours before the experiments and not to eat or drink (larger than 1 dl) one hour before each study protocol. The experiments were generally performed in 1 day between 8 am to 7 pm in a quiet room with normal ambient temperature. All participants provided written informed consent (ClinicalTrials.gov registration identifier NCT02268266).

2.3 Experimental protocols

The study consisted of four different study protocols (i.e., 12 experiments) resulting in 4 h and 24 min of recorded data from each subject. The protocols were designed based on step inputs (see below, Sect. 2.4.7). The order of the protocols was not randomized. However, the time intervals between the protocols were so long, that they were considered independent. Before each experiment, the subject was fixed to the tilt table using the provided harness and the tilt table was adjusted to the subject's height. To minimize disturbances entering the cardiovascular system, during the measurements the subjects were asked not to talk unless in the case of a discomfort requiring experiment interruption. Furthermore, the subjects were asked to relax and stay passive during the experiments to ensure the minimum muscle activity during the protocols involving stepping [46]. The CNAP® monitor was calibrated every time before running an experiment. An initial 5-min rest period was considered at the beginning of each experiment to minimize any effects from the calibration or previous experiments. Part of the data recorded during the experiments was already analyzed for another study with a focus on overall observable patterns in cardiovascular responses [37], where we also reported the corresponding parts of the protocols. Here, we present the complete course of experimental protocols and examine all the recorded data to investigate subject-specific modeling of the relationship between the external stimuli and the cardiovascular variables.

2.3.1 Inclination angle (study protocol 1)

The goal of this study protocol was to identify models describing the inclination angle effect on HR, sBP and dBP. In a first step, the subjects were tilted to the maximum tilt angle $\alpha = 71°$ and then to $\alpha = 40°$ with a 3 min supine period in between (see Fig. 1b). In a second step, the same experiment was conducted with $\alpha = 60°$ instead of $\alpha = 71°$ to make the potential input nonlinearity visible. A full tilt up or tilt down between supine and maximum tilt angle takes approximately 20 s depending on the load and its duration can be upper bounded by 30 s. Thus, the step-up and step-down phases in this protocol were, in fact, a ramp-up–constant–ramp-down sequence, where the constant phase was longer than the ramp times so that it could be approximated with a step.

2.3.2 Stepping without and with FES (study protocols 2 and 3)

Study protocols 2 and 3 were considered for identifying the stepping effect without FES and with FES, respectively, on HR, sBP, and dBP. The effects on the outputs are driven by the underlying exercise of such activity (e.g., 48 steps per minute stepping exercise). A 5 min phase of stepping with 48 steps per minute was followed by a 5-min rest period and 5-min stepping with 36 steps per minute (see Fig. 1c), where for comparative reasons the stepping frequency was chosen in a similar range as considered in [45, 47]. The change in the position of the legs and their movement occurs so quickly after a change in the input signal that step-up and step-down phases in the stepping frequency in these protocols could be assumed instantaneous. Both protocols were conducted at $\alpha = \{20°, 40°, 60°\}$ of tilt (three experiments per protocol) in a random order. Since the tilt table was adjusted to the height of the subject, a meaningful range of motion for the legs could be guaranteed during the passive stepping performed in the protocols.

Using the FES module of the tilt table, the muscles of the legs can be stimulated according to a walking pattern, i.e., during leg extension Mm. quadriceps femoris and tibialis anterior are stimulated, whereas during flexion the Mm. biceps femoris and gastrocnemius. To produce a tetanic (i.e., sustained and smooth) muscle contraction while avoiding early fatigue, the FES frequency was set to 40 Hz [47]. The FES pulse was bipolar and biphasic with a width of 300 μs and its amplitude could be varied between a minimum (I_{MIN}) and a maximum (I_{MAX}). We determined these two values before the experiments individually for each subject per muscle group similar to the approach used in [47] and they were between 7 and 30 mA (see Supplementary Material, Chapter 1 for details). The minimum amplitude (I_{MIN}) was defined as the minimum current I inducing a visually detectable muscle contraction and was the current applied in protocol 3. The maximum amplitude (I_{MAX}) was set according to the maximum tolerable stimulation amplitude by the subject. To ensure safe and comfortable application, only $\xi = 80\%$ of the I_{MAX} was finally applied in the study protocols. The FES current amplitude can, therefore, be calculated as follows:

$$I_{\mathrm{FES}} = I_{\mathrm{MIN}} + u_{\mathrm{FES}}(\xi I_{\mathrm{MAX}} - I_{\mathrm{MIN}}), \tag{1}$$

where I_{FES} is the applied current amplitude, I_{MIN} and I_{MAX} are the identified thresholds, $u_{\mathrm{FES}} \in [0, 1]$ is the FES input and $\xi = 80\%$ a safety factor. The change in the FES current occurs so fast after a change in the input signal that a step-up or a step-down phase in FES current amplitude could be considered instantaneous.

2.3.3 FES amplitude (study protocol 4)

The aim of this study protocol was to identify the effect of the change in FES amplitude during the stepping with FES on the cardiovascular variables. A 5-min synchronized stepping with minimum FES input was applied ($u_{\text{FES}} = 0$, i.e., I_{MIN}) followed by a 5-min interval of maximum FES input ($u_{\text{FES}} = 1$, i.e., $0.8I_{\text{MAX}}$) and a 5-min period during which the amplitude was set back to minimum current strength (see Fig. 1d). Since a prolonged FES application could result in muscle fatigue [20], potentially affecting the results, the inclusion of a second step input in this study protocol was omitted. The protocol was conducted at four different tilt angles $\alpha = \{0°, 20°, 40°, 60°\}$ (four experiments) in a random order.

2.4 System identification

2.4.1 Problem formulation

As described before (see Sect. 1), we aimed at identifying *low-order* models. To this end, we considered identification of first- or second-order *linear* TFs G and compensating encountered nonlinearities through a Hammerstein model structure [2] (i.e., a memory-less nonlinearity followed by a linear TF, see Fig. 2). Hammerstein models are widely used in modeling physiological processes (e.g., [23, 24, 43]) and are already applied in development of cardiovascular biofeedback systems (e.g., [14, 43]). Using a Hammerstein model could also simplify the controller design later by providing the possibility to use existing linear control approaches after inversion of the memory-less nonlinearity part of the model [43]. The goal was to obtain the nonlinear part of the model using basis functions estimated from the data of a sample population, and identify the linear TFs individually for each person. Since HR and BP are discrete events, discrete-time identification for the linear TFs is suitable, and the problem could be formulated as (see Fig. 2):

$$\mathbf{y} = G(\theta, z)\mathbf{u} + \mathbf{v} \tag{2}$$

where $\mathbf{y} = \begin{pmatrix} y_1 & y_2 & y_3 \end{pmatrix}^\top = \begin{pmatrix} \text{HR} & \text{sBP} & \text{dBP} \end{pmatrix}^\top$ is the system output, $\mathbf{v}$ noise, $G(\theta, z)$ the discrete-time linear TF to be identified, and $\mathbf{u}$ the transformed input using the nonlinear mapping:

$$\mathbf{u} = \mathbf{f}(\bar{\mathbf{u}}) = \begin{pmatrix} u_1 & u_2 & u_3 \end{pmatrix}^\top \tag{3}$$

with $\mathbf{f}(\cdot) = (f_1(\cdot)\, f_2(\cdot)\, f_3(\cdot))^\top$ to be the static mapping vector including the corresponding nonlinear functions (representing nonlinearity in Fig. 2) and

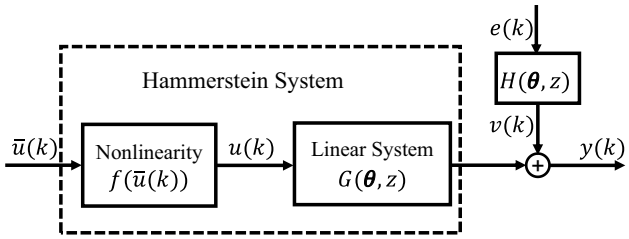

Fig. 2 Hammerstein model structure consists of a static nonlinearity followed by a linear dynamic system. Based on general linear model structure assumption, the output of the linear part is corrupted by noise $v(k)$ which is the output of the stochastic TF $H(\theta, z)$ under white noise input $e(k)$

$$\bar{\mathbf{u}} = \begin{pmatrix} \alpha & f_{\text{step}} & u_{\text{FES}} \end{pmatrix}^\top \tag{4}$$

to be the original untransformed input with α, f_{step}, and u_{FES} representing the input values for inclination, stepping frequency, and FES, respectively. It is to note that the response to stepping frequency f_{step} could be identified in two variations (without or with FES, i.e., study protocols 2 and 3).

2.4.2 Nonlinearity

Obtaining a nonlinearity for each subject individually in a short identification phase before the biofeedback therapy is practically infeasible. Thus, a nonlinear mapping $\mathbf{f}(\cdot)$ is introduced beforehand for all people such that it is enough to estimate one data point in the identification phase to infer the whole nonlinearity. The nonlinear part of the Hammerstein model is estimated using the data from the sample population rather than the subject-specific data.

It is reported that in tilting from supine to 90° most changes happen between 20° and 60° [22, 29] and in this range they are linearly related to the angle of tilt [22]. Therefore, the nonlinearities between HR, sBP and dBP, and the inclination angle were approximated using a logistic sigmoid function:

$$f_{\text{sig}}(\alpha) = b\left(\frac{1}{1 + e^{-a(\alpha - c)}} - \frac{1}{1 + e^{ac}}\right) \tag{5}$$

with parameter values $a = 0.0957$, $b = 1.04438$, and $c = 40$. This function maps the inclination angle range between 0 and about 1, such that $\alpha = 40°$ corresponds to the half-value (0.5) and a slope of 1/40 preserves rather a linear relationship between 20° and 60°. Accordingly, $f_1(\bar{u}_1) = f_1(\alpha) = f_{\text{sig}}(\alpha)$ (see Eqs. 3, 4). Since no information could be found from the literature about nonlinearities of stepping and FES inputs, in this initial stage only identification of the linear part of the response to these inputs

was considered. Thus, it was assumed that $f_2(\bar{u}_2) = \bar{u}_2$ and $f_3(\bar{u}_3) = \bar{u}_3$.

2.4.3 Linear system

Having three inputs and three outputs, for the linear part of the system an individualized linear discrete-time MIMO model G consisting of 9 TFs G_{ij} was considered, where G_{ij} is the TF from input j to output i.

To identify each single TF, the inputs were perturbed one at a time (see Sect. 2.3). The outputs were measured and then the TFs from each specific input (e.g., inclination α) to all the outputs (i.e., HR, sBP and dBP) were identified. The procedure was repeated for all the three inputs (in the case of f_{step} for both without and with FES conditions). A single discrete-time linear TF can be written as [27]:

$$G_{ij}(\theta, z) = \frac{B(\theta, z)}{A(\theta, z)}, \tag{6}$$

where

$$A(\theta, z) = \sum_{i=0}^{n_a} a_i z^{-i} = 1 + \bar{A}(\theta, z) \tag{7}$$

$$B(\theta, z) = \sum_{i=0}^{n_b - 1} b_i z^{-(i+n_k)} \tag{8}$$

$$\theta = \left(a_1, \ldots, a_{n_a}, b_0, \ldots, b_{n_b - 1}\right) \tag{9}$$

with n_a as order of the denominator, n_b order of the numerator and n_k the number of dead-time samples corresponding to the time delay. Z represents z-transform.

Although the goal was to identify low-order models, it was still desired to capture dynamics describing exponential adaptations or overshoots in response to the external stimuli. In continuous time domain, this can be achieved through first- or second-order models, respectively. In discrete-time domain, counterpart first- and second-order models can be captured with $n_a = 1, n_b \in [1, 2, 3]$ and $n_a = 2, n_b \in [1, 2, 3]$, respectively (assuming bilinear transformation [41]). Therefore, we investigated identification of models up to $n_a = 2$ and $n_b = 3$. We expected that the reaction would not be delayed more than 30 s and for the estimation of time delay n_k, a resolution of about 1 s was considered acceptable. Thus, considering the sampling time 0.3 s, for the estimation of time delay $n_k \in [0, 100]$ in steps of 3 samples was investigated in the identification procedure (see below, Sect. 2.4.5). To fit the linear TF G, the ARX and OE structures were considered [27]. These linear model structures assume that the measured output is equal to the true output plus a noise signal $v(k)$, being the output of a noise model $H(\theta, z)$ with a white noise input $e(k)$ (see Fig. 2). ARX assumes the noise model to be $H = \frac{1}{A(\theta,z)}$, whereas OE assumes simply $H = 1$. The parameters θ, which define the TF $G(\theta, z)$, are estimated by minimizing the squared sum of all errors $e(k)$.

2.4.4 Offset handling

Model structures such as ARX or OE can only capture the variations in the outputs caused by the applied inputs, and therefore, in the identification procedure the observed offset in the outputs needs to be accounted for separately. A constant offset can be handled in two ways; (1) by detrending the output biosignals before the identification; (2) by including the offset directly into the optimization stage of the identification.

The first approach was implemented by simply considering the mean of the signal as offset and subtracting it from the original signal. For the second method, which was only applied in the context of ARX, similar as in [21] an affine transformation was used. By subtracting the offset d from the output, a normal ARX structure for the difference can be considered:

$$A(\theta, q)(y(k) - d(k)) = B(\theta, q)u(k) + e(k), \tag{10}$$

where $y(k)$, $u(k)$, and $d(k)$ are the measurement, input, and the offset at each time step k, and q (replacing z) represents the system in time domain.

Since $d(k) = d = \text{const.}$, the equation can be rewritten as:

$$A(\theta, q)y(k) = B(\theta, q)u(k) + \left(1 + \sum_{i=1}^{n_a} a_i\right) \cdot d + e(k) \tag{11}$$

which can be reformulated as a standard least squares problem:

$$\mathbf{y} = \boldsymbol{\Phi} \cdot \mathbf{x} + \mathbf{e}, \tag{12}$$

where each row represents a data point, and is of the form:

$$\begin{aligned} y(k) = [&-y(k-1), \ldots, -y(k-n_a), \\ &u(k-n_k), \ldots, u(k-n_k-(n_b-1)), 1] \cdot \mathbf{x} + e(k) \end{aligned} \tag{13}$$

where

$$\mathbf{x} = [a_1, \ldots, a_{n_a}, b_0, \ldots, b_{n_b-1}, c]^\top \tag{14}$$

$$c = \left(1 + \sum_{i=1}^{n_a} a_i\right) \cdot d \tag{15}$$

With sufficient measurements, the least squares problem can be solved to obtain the parameters $\mathbf{x}$. Then the offset

d is calculated by transforming the parameter c using Eq. 15. We refer to this approach as Offset-free ARX (OARX) because the offset is handled directly within the method.

Thus, based on the offset handling approaches, three different model structures were investigated; (1) ARX with offset compensation using optimization (OARX); (2) ARX with detrending (referred as ARX); (3) OE with detrending (referred as OE).

2.4.5 *Identification framework*

The identification framework was as follows:

(a) The data from each experiment were divided into two parts (see Fig. 3): (1) Training and validation set (identification set); (2) Testing set. The training and validation set was used to construct the model for each cardiovascular variable, whereas the testing set was not touched in any step of the identification procedure. For study protocols 1, 2 and 3, and 4, the data between 240–540, 60–800, and 480–960 s (highlighted areas in Fig. 1b–d) were used as training and validation set, respectively. These time periods were chosen such that both step-up and step-down phases (square-wave signal) of the response to the external stimuli were included (see below, Sect. 2.4.7). For the testing set, the data after the training and validation set until the end of the corresponding protocol was used.

(b) K-fold cross-validation technique [6] with $K = 10$ was used to divide the training and validation set into two parts (see Fig. 3): (1) training set; (2) validation set. $K - 1$-folds were considered as the training set and ν-th-fold was considered as the validation set (see Fig. 3).

(c) Training set was used to train models based on combinations of model structures (OARX, ARX, OE), model orders $n_a \in [1, 2]$, $n_b \in [1, 2, 3]$, and time delays $n_k \in [0, 3, 6, 9, \ldots, 99]$ (see Sect. 2.4.3), resulting to $3 \cdot 2 \cdot 3 \cdot 34 = 612$ estimated models for each cardiovascular variable. However, evaluation of the identification framework in simulation revealed that for first-order systems OARX and ARX can estimate the output well even if the model structure differs from the noise model assumptions, whereas for second-order systems OE might be required as well (see Supplementary Material, Chapter 2). Therefore, for computational efficiency, the OE model estimation was only performed for second-order systems (i.e., $n_a = 2$ and $n_b \in [1, 2, 3]$). This reduced the number of models to be estimated from 612 to 510.

(d) The validation set was used to evaluate different model orders and time delays for each model structure. The outputs of the already estimated models from the training set were simulated, and the root-mean-square error (RMSE) and coefficient of determination (R^2) [30] between the simulated response and the measured response (3.3 Hz, unfiltered) of the validation set was calculated.

(e) The steps (c) and (d) were repeated over all possible combinations of $\nu \in [1, \ldots, K]$ such that each fold was considered once as the validation set (K-fold cross-validation [6], for implementation details, see below, Sect. 2.4.6). The model order and time delay with the lowest average RMSE were selected for each model structure. To avoid overfitting a higher model order was only selected when the RMSE was decreased by more than 5% per model order ($n_a + n_b$). This resulted in three models with three different structures OARX, ARX, and OE. Then, for each model the median of the calculated R^2 values in the cross-validation was compared with $R^2 = 0$. If $R^2 < 0$ the model was replaced with the mean model (i.e., considering mean of the data as the model). This resulted in three models which could be an OARX, ARX, OE, or mean model.

(f) Before selecting the best model describing the data, in a first step, the parameters of each model with already determined order and time delay were retrained on whole the training and validation set (identification set). This approach trained the models on more data, and therefore, it was expected that it results in a better fit. Then, for further improvement of estimated model parameters in the case of the OARX and ARX structures, an additional step of the instrumental variable method was also performed. The instrumental variable method allows consistent and unbiased estimation of model parameters [27]. As instruments, the simulated output of each model was used, and the model parameters were re-estimated.

(g) At this stage, we still had three models. However, the models that had unreasonable settling time (more than 180 s for inclination and 300 s for other inputs)

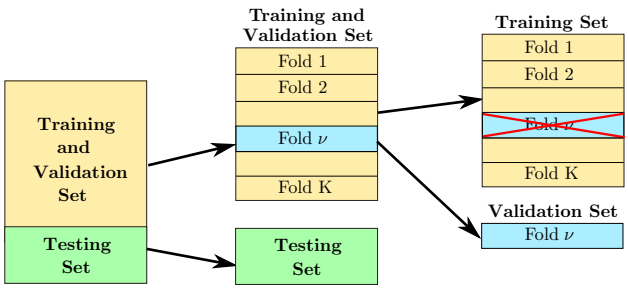

Fig. 3 Data flow of the identification procedure with K-fold cross-validation

were detected and rejected. If all the models were rejected, the mean of the data was considered as the final identified model. Otherwise, the RMSE between the simulated output and the *filtered* output (see below, Sect. 2.4.8) on the identification set was calculated for each model, the higher model orders were penalized by adding 5% extra error per model order ($n_a + n_b$) to their newly calculated RMSE and finally, the model with the minimum error was selected as the final model.

(h) To evaluate the reliability of the final selected model in response prediction, the evaluation had to be done on a different set than the set used for pattern recognition and model training [6]. Thus, the selected model was used to predict the response in the testing test, which was not utilized before (see Fig. 3), and the R^2 coefficients based on the filtered measured signal (see below, Sect. 2.4.8) was computed and reported.

2.4.6 Implementation of K-fold cross-validation

The OARX and ARX structures can be formulated as standard regression problems. Thus, implementation of the K-fold cross-validation for these approaches can be discussed more rigorously than the OE structure. In the OARX and ARX approach, each measurement sample provides one row (see Sect. 2.4.3, Eq. 13). If we stack all rows corresponding to the measurements, a standard least squares problem is obtained. Thus, each row can be either put into the training set or be used in the validation set. Omitting the first n_k samples to consider the time delay in the model, $N - n_k$ rows were split into K folds and the K-fold cross-validation procedure (see Sect. 2.4.5) was followed. The only limitation of this approach was that since each output and input are present in different rows ($y(k)$ is in n_a different rows and $u(k)$ in n_b rows), the rows were related. This means that the validation and training set were not completely independent. However, since only small model orders n_a were considered and relatively a high number of samples were available, the overlap between the training and validation set was small and therefore, the dependency could be neglected.

For the OE structure, the inputs and outputs were split into K sets and cross-validation was conducted; the ν-th set was selected for validation and the rest $K - 1$ sets were stacked together as the training set. This approach could be more problematic than the one implemented for OARX and ARX models, which could be formulated as a least squares problem. When the inputs and outputs are stacked to form the training set, they are put differently together. This can introduce a discontinuity (a jump in the output values) in the data which in a linear regression task might result in a biased estimate of the model parameters [25]. However, since K and the number of samples N were relatively large, we did not expect that a drastic jump would occur and influences the result significantly.

2.4.7 Input design

The input design plays an important role in the system identification. In our approach, we designed step inputs for identification. A simple step, however, is not qualified. Due to hardware issues as well as physiological mechanisms, asymmetry in the responses, when the same amount of stimuli in opposite direction is applied, could happen. In fact, physiological responses are very often asymmetric, for example, in the case of inclination input, Toska and Walløe [44] describes that for a tilt up, most changes occur during the first 30 s after the tilt, whereas for a tilt down, changes take place within 10 s. Therefore, for the identification set we included both step-up and step-down phases (square-wave signal) to get the best average fit (see highlighted areas in Fig. 1).

To decide the length of step input for the inclination input, some guidelines could be found in literature [40, 44]. These studies suggest that most hemodynamic changes to the upright posture happen during the first 30 s. The inclination ramp-up to 71° takes about 20 s depending on the load and its duration can be upper bounded by 30 s. Considering the 30 s upper bound for tilting and adding 90-s extra time to the initial 30-s settling time to allow the system to get even closer to steady state, a total time of 150 s for the inclination angle square-wave was considered. This period started at the beginning of the ramp-up and ended at the beginning of ramp-down, and therefore, in reality, the square-wave including ramp-down took about 180 s. No scientific study could be found about the response time for stepping and FES; however, based on the responses observed in some previous studies [45] a square-wave input of 300 s was considered acceptable.

There are many other popular input types such as pseudorandom binary sequence (PRBS) or frequency sweep that could be used for identification (e.g., [14, 43]). Three reasons motivated our choice for a step input: (1) When dealing with human subjects, alternating inputs such as PRBS might be undesirable due to subject's discomfort or associated clinical risks. (2) More importantly, these alternating inputs are not always ideal for identification of a nonlinear system such as the human cardiovascular system. For example, PRBS input, although ideal for linear system identification, is not suitable for nonlinear system identification. PRBS input can cause loss of identifiability [26], as its amplitude changes between two levels and therefore, it may

linearize the nonlinear system dynamics and not be persistently exciting [5]. A similar argument can be made for a step input. Nevertheless, a PRBS input can be quite beneficial for nonlinear system identification, when two-step (independent linear and nonlinear part) identification of a Hammerstein model is considered. This input type can decouple the linear and nonlinear part of the system, and turn identification of the Hammerstein model into a linear problem respecting the same convergence and consistency results in the absence of unknown nonlinearity [2]. This enables application of any linear system identification method for estimation of the linear part of the Hammerstein model [2]. Following a similar proof as in [2] it can be shown that this benefit also holds for a step input (see Supplementary Material, Chapter 3 for details). In contrast to a PRBS or a step input, the output of other input types such as a frequency-sweep signal might also include system nonlinearities, and therefore, their application in the context of two-step identification of the Hammerstein model structure (e.g., as in [14]) can be considered inefficient and error prone. (3) The focus of most cardiovascular biofeedback systems including ours is the steady-state (i.e., DC gain of the TFs) rather than the transient behavior of the cardiovascular variables (e.g., [13, 14, 36, 42, 45]). For a step input, more energy is assigned to lower frequencies and in particular DC gain. Therefore, considering the limited identification time when dealing with human subjects, and thus, the constrained amount of energy transfer to the plant, a step input was more suitable as it could emphasize the DC gain more.

2.4.8 Filtering of the signals

The originally measured signals (3.3 Hz) contained variability that was out of interest, and thus, it could be considered as noise. Therefore, since the goal of the estimated models was to describe long-term dynamics of the cardiovascular variables, the evaluation of the models in the last two steps of the identification framework (steps g and h, see Sect. 2.4.5) were done on the *filtered* measured signals. To filter the signals, the source of variability in the signals had to be considered. The oscillations of the HR and BP can be divided into three ranges based on their source: (1) Natural oscillations in the range 0.02–0.4 Hz consisting of oscillations of 0.02–0.07 Hz related to cardiorespiratory phenomena, around 0.1 Hz produced by Mayer waves, and 0.2–0.4 Hz produced by normal respiratory activity [33]. (2) Adaptation to external stimuli such as inclination, stepping and FES in the range from seconds to minutes [40, 44]. (3) Slow changes in the range of hours and days due to changes in the blood volume, hormonal changes, etc. To consider the long-term dynamics caused by the external stimuli, the mean changes in the signal needed to be considered and fast dynamics had to be filtered. The signals were low-pass-filtered using a moving average filter with a length of 40 s and the time stamp was shifted such that no delay was introduced. With a sampling time of 0.3 s, this filter length corresponds to a cutoff frequency at 0.01 Hz and almost a complete attenuation of the signals from 0.02 Hz on.

2.4.9 Signal-difference-to-noise ratio

To measure how much the externally-induced patterns differed from natural oscillations in the cardiovascular variables, the signal-difference-to-noise ratio (SDNR) [4] was applied in the context of the biosignals (see Supplementary Material, Chapter 4 for details). Due to very low SDNR values observed in the study protocol 4 and high probability of overfitting, the identification of second-order models for this study protocol was omitted.

2.5 Data processing and statistical analysis

For signal analysis MATLAB® R2014 (MathWorks Inc., Natick, MA, USA) was used. To evaluate the overall prediction performance of the identified models, R^2 coefficients evaluated on the testing set (see step h in Sect. 2.4.5) in the case of each experiment were compared with $R^2 = 0$ statistically. Since R^2 is maximally 1, but has no limit on the minimum and can thus even become negative, we did not expect that computed R^2 coefficients have a normal distribution. Therefore, for the evaluation of R^2 coefficients nonparametric statistical tests were utilized. Accordingly, a one-sample Wilcoxon signed-rank test [39] with respect to $R^2 = 0$ was used to compare whether the overall prediction performance of the models in each case is better than taking the mean of the signal or not. Note that this mean is the average of the testing set, which is not accessible in advance, and thus $R^2 = 0$ cannot trivially be obtained by taking a mean at model generation step. In the case of inclination input, Wilcoxon signed-rank test was performed to compare R^2 values without and with the proposed sigmoid nonlinearity (see Sect. 2.4.2) and to analyze whether consideration of this nonlinear function systematically leads to higher R^2 values. For each cardiovascular variable, the analyses were done independently. To compare the performance of different model structures in modeling the experimental data (i.e., training and validation set), the number of identified models in each model structure was compared using the Chi-squared test. The statistical analyses were done with IBM SPSS Statistics (version 22.0, Armonk, NY: IBM Corp.) and the minimum significance level was set at $p = 0.05$.

3 Results

The structure, order, and gain of identified TFs from the experiments together with the corresponding R^2 coefficients and SDNR values for each subject are reported in the Supplementary Material, Chapter 5.

3.1 Prediction performance

The one-sample Wilcoxon signed-rank test showed that only in some cases for inclination and stepping without FES, the identified models were systematically reliable (see statistically significant findings in Table 2). For inclination, the HR TFs in 60° and 71° experiments were able to explain 65.5 and 74.0% of the observed variance in the data, respectively. The inclination sBP and dBP TFs performed much worse. The sBP TFs were only reliable when obtained at 71° experiment (explaining 29.4% of the observed variance) and the dBP TFs only when obtained at 60° experiment (explaining 35.6% of the observed variance). Although a high prediction performance (78.5% explained variance) was also observed in the obtained dBP TFs for inclination input at $\alpha = 71°$ experiment, due to some extreme cases, this performance was not statistically significant, and it was, therefore, unreliable. The other reliable identified models were only the sBP TFs for stepping without FES at 40° experiment explaining only the negligible amount of 3.9% of the observed variance. Furthermore, in two cases (sBP and dBP TFs at 40° experiment for FES amplitude) it was observed that the models systematically perform worse than the mean signal of the testing set. The computed R^2 values for FES amplitude TFs only evaluate the model in no FES input part. Therefore, low prediction performances for these TFs imply that we even have problem to predict the testing set data offset, i.e., when we change back the FES amplitude input from $u_{\mathrm{FES}} = 1$ ($0.8I_{\mathrm{MAX}}$) to $u_{\mathrm{FES}} = 0$ (I_{MIN}), the response does not necessarily go back to the initial observed steady-state value at $u_{\mathrm{FES}} = 0$ before applying the stimulus.

3.2 Observable patterns

For the inclination input, HR and dBP gains were always positive, while the gain direction for sBP was more diverse (see Supplementary Material, Chapter 5). This observation is in agreement with the well-documented literature of tilt table experiments which is well discussed before for physiological modeling approach presented before [45]. A sample response is shown in Fig. 4. In most cases (8 out of 10 subjects), HR and dBP responses were monotonically positive, i.e., by increasing the angle from 60° to 71° also the gain values increased.

The identified TF for stepping without and with FES, as well as FES amplitude were different at each inclination angle. To exemplify this phenomenon, a single subject sample responses to stepping without FES at 20° and 40° are presented in Fig. 5. In this specific example, it can be observed that for the HR the system order changes over the angle (second-order OE model at 20° (see Fig. 5A-a) versus first-order ARX model at 40° (see Fig. 5B-a)), and for sBP and dBP, the responses are different at each angle (no response (mean model) at 20° (see Fig. 5A-b, c) versus

Table 2 One-sample Wilcoxon signed-rank test analysis of R^2 coefficients (test value $R^2 = 0$)

Cardiovascular variable		HR			sBP			dBP		
Input	Experiment	Mdn	Z	p value	Mdn	Z	p value	Mdn	Z	p value
Inclination	60°	0.656**	2.803	0.005	0.110	0.561	0.575	0.356**	2.599	0.009
	71°	0.740**	2.803	0.005	0.294*	1.988	0.047	0.785	1.274	0.203
Stepping	20°	−0.006	−1.178	0.859	0.001	0.059	0.953	−0.033	−1.481	0.139
	40°	−0.004	0.296	0.767	0.039*	2.192	0.028	0.012	0.255	0.799
	60°	−0.006	−0.764	0.445	0.102	0.968	0.333	−0.038	−1.718	0.086
Stepping + FES	20°	−0.020	−0.357	0.721	0.005	0.102	0.919	−0.052	−1.172	0.241
	40°	0.002	0.153	0.878	−0.000	0.051	0.959	−0.010	−0.663	0.508
	60°	0.146	1.580	0.114	−0.016	−0.561	0.575	−0.015	−0.663	0.508
FES amplitude	0°	−0.003	0.153	0.878	−0.013	−1.481	0.139	0.000	−0.459	0.646
	20°	0.001	0.051	0.959	−0.002	0.255	0.799	−0.012	−0.459	0.646
	40°	−0.313	−1.478	0.139	−0.248*	−2.293	0.022	−0.026*	−2.429	0.015
	60°	−0.052	−0.459	0.646	−0.006	−1.601	0.109	0.003	1.429	0.153

Mdn stands for median of the R^2 values of the identified models in the corresponding experimental condition. p values correspond to 2-tailed asymptotic p values. The signs * and ** show significant findings with p values ≤0.05 and 0.01, respectively

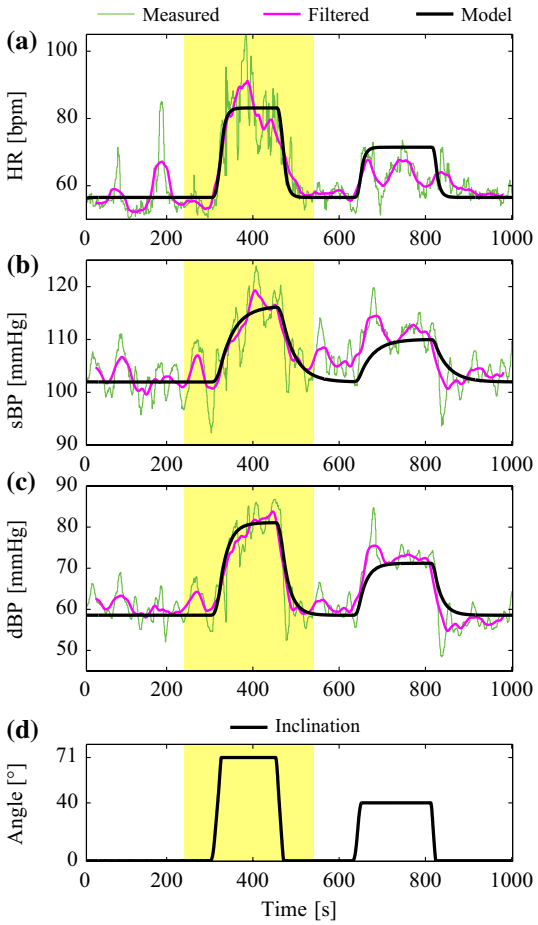

Fig. 4 HR, sBP, and dBP responses (**a**–**c**) of subject 7 in response to angle input (**d** $\alpha = 71°$ experiment) together with simulated responses based on the identified models. The *highlighted areas* show the data range used for the identification of the corresponding model

first-order ARX model at 40° (see Fig. 5B-b, c), respectively). In some cases even the gain direction (i.e., the sign of the TF) changes over the angle (e.g., in HR response of 6 out of 10 subjects to stepping without FES). This result is also supported by the sign of the SDNR values which in some cases change between negative and positive values by changing the inclination angle. These observations imply that stepping without and with FES, as well as FES amplitude are coupled with the inclination input and in some subjects, a zero-crossing exist.

For the stepping without FES, the sBP responses are ordered such that often the DC gains show a positive monotonic behavior over the angle (7 out of 10 subjects), i.e., the gain never becomes more negative for higher inclination angles. The responses for stepping with FES were more diverse than stepping without FES. No particular pattern in the estimated models for FES amplitude was observed.

3.3 Performance assessment in experiments

In total 360 TF were estimated from which 246 are first-order, 30 second-order, and 84 mean models. From the 246 estimated first-order models, 165 cases are in the ARX structure and 81 cases in the OARX structure. Accordingly, the first-order TFs showed a statistically significant tendency toward the ARX structure rather than the OARX structure, $\chi^2(1, N = 246) = 28.683$, $p < 0.001$. All the identified second-order TFs are in the OE structure, and no second-order model with ARX or OARX structure was selected based on the defined criteria in the identification framework. The percentage share of each model structure in the identified models is presented in Fig. 6. It is to note that the structure comparison is only based on training and validation set, i.e., which structure is well suited for modeling the observed data in this set.

Excluding the identified models for FES amplitude, where we only focused on first-order models, the identified models for other protocols show that most often a first-order TF is sufficient to describe the cardiovascular system behavior with respect to the applied external stimuli in the training and validation set (70.1% of the 240 models), and only in case of HR response to stepping without FES a second-order system might be necessary to model the overshoot of 5–10 bpm observed in about 30% of the corresponding experiments (see Fig. 6). Figure 5A-a demonstrates such a case where the HR response description requires a second-order model. In the case of stepping with FES such an overshoot was also observed, however in about 20% of the cases (see Fig. 6).

4 Discussion

4.1 Identified models and prediction performance

SDNR values revealed that for the inputs except the inclination input, the steady-state change is as big as the natural oscillations and in the case of FES amplitude even smaller. This result implies that in general modeling of the responses to the inclination input is easier than the other input types. In particular, the observation generally holds for these inputs, since the intensity levels that we used for the input stimuli cover a substantial extent of the available ranges and thus, the corresponding SDNR values cannot be increased significantly. For example, in the case of inclination, we tested both 60° and 71° (maximum inclination). For stepping without and stepping with FES, we tested these inputs at tilt angles up to 60° and at frequencies more than half of the available range (48 steps per minute of the maximum possible 80 steps per minute). For FES,

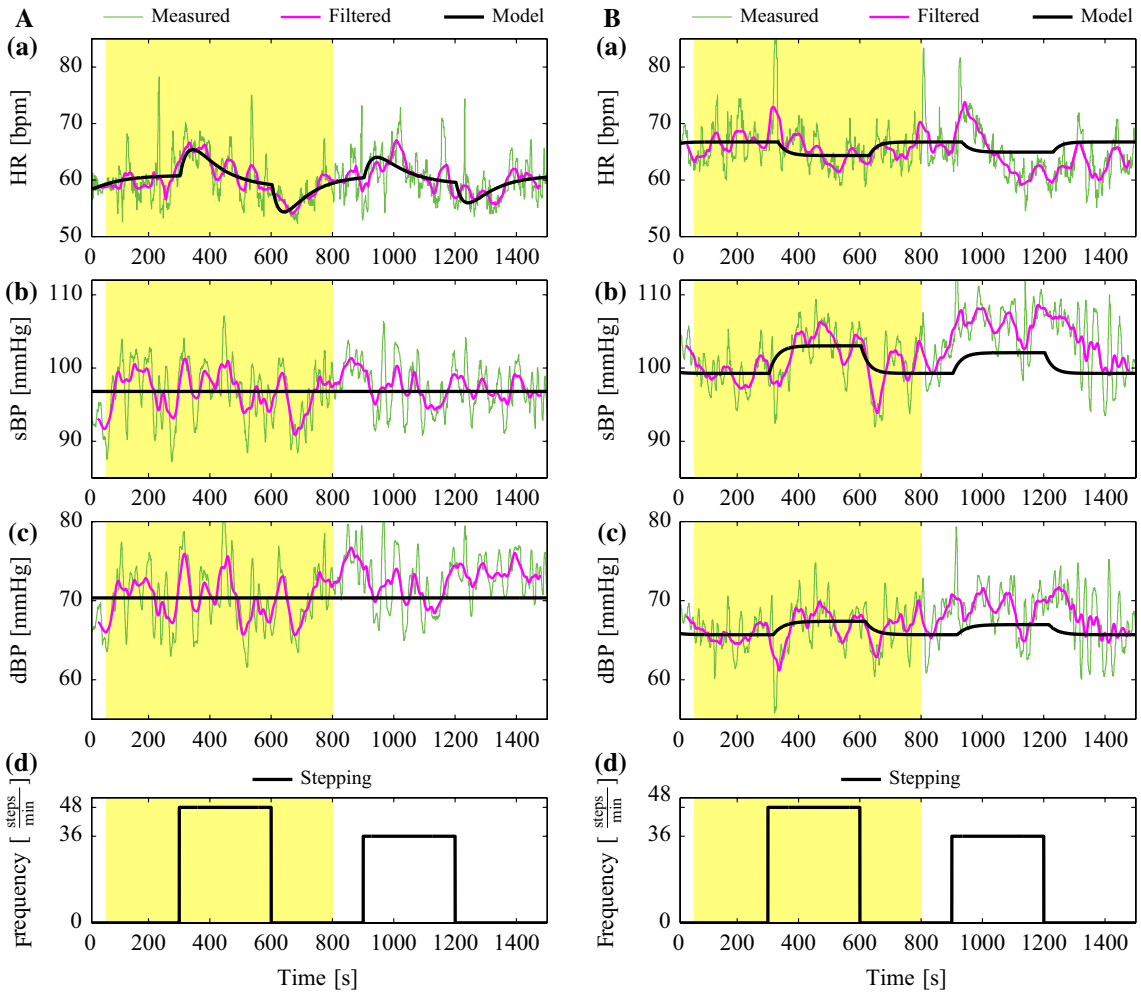

Fig. 5 HR, sBP, and dBP responses (**a**–**c**) of subject 7 in response to stepping input (**d**) at 20° (column A) and 40° (column B) together with simulated responses based on identified TF models. The *highlighted areas* show the data range used for the identification of the corresponding model

we considered up to 80% of the maximum available range (pain threshold of the subjects).

The comparison of the computed R^2 values based on the testing set with $R^2 = 0$ answers the question whether the identified models systematically perform better than the case when we could access the testing set in advance and had considered the mean signal as a model. This simply means to what extent the identified models are systematically reliable to predict the responses when dealing with unseen data. We observed that only the identified models for HR response to inclination input can explain the observed variance in the data to a reasonable extent (on average 69.8%) and the other identified models either are not reliable or in general explain a negligible amount of the observed variance (maximum up to 35.6%, dBP TFs for inclination input at $\alpha = 60°$ experiment). Therefore, only in case of HR response to inclination input, reliable models with acceptable prediction performance for control system design could be achieved.

The low prediction performance of the identified models is not necessarily due to inappropriate modeling assumptions or the identification procedure, but rather due to the complexity of the system at hand, ignored nonlinearities, and the difference in the nature of the reaction in the identification and testing set. For inclination input, for example, such a difference in the nature of reaction can be observed for sBP and dBP in Fig. 4b, c, where these variables in response to 40° of tilt (testing set, 540 s onward) show rather a second-order behavior with observable overshoots, instead of a first-order behavior, which is identified based on the identification set. These changes in behavior might be explained when we note that the cardiovascular responses are mainly controlled by baroreflex control [38], i.e., the human body internal controller, which we aim at

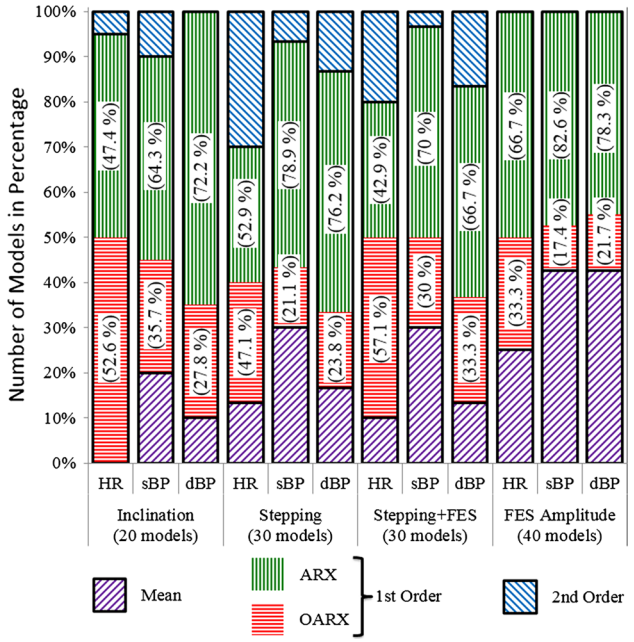

Fig. 6 The frequency of the order of the identified TFs in each study protocol. For first-order models, the percentage share of OARX and ARX is also shown

augmenting it with an external closed-loop controller. The set point of the baroreflex controller might be changed, for example, even by changing the inclination angle [38]. These potential changes in set point or adaptation strategies governed by the baroreflex circuit might explain why the nature of reaction in the identification and testing set is different, and consequently, why the introduced nonlinearity for inclination input did not improve the prediction performance significantly.

Low prediction performance of the models obtained for other inputs (i.e., stepping without FES, stepping with FES, and FES amplitude), besides set point changes, might be explained by potential nonlinearities existing in response to these stimuli. Such a nonlinearity can be observed for example in sBP response to stepping input of subject 7 at $\alpha = 40°$ tilt (see Fig. 5B-b), where 36 steps/min (testing set) in comparison with 48 steps/min (identification set, i.e., highlighted area in Fig. 5B-b) results in higher increase of sBP.

Furthermore, in some cases, change in the direction of the gain was observed by changing the inclination angle, i.e., for the same input type and the same intensity, the direction of the change might be different at each inclination angle. Here, although the gains are rather small in some cases and can be considered as oscillations around a set point considered by the baroreflex circuit, it can be said that for some subjects, a zero-crossing over the angle happens. To design a stable controller, the zero-crossing needs to be detected, as, without this knowledge, it would not be clear at each inclination angle, the input change in which direction has to be provided to move the cardiovascular variables toward the desired ranges. However, detection of such a zero-crossing might not be possible without extensive experimental tests which might be infeasible due to associated risks.

These results were observed in a healthy population with healthy baroreflex responses, whether they hold for patients with impaired baroreflex circuit, and altered reflex responses [1], needs further investigation. Moreover, in contrast to a healthy population, the applicable inputs can be more restricted in our target population consisting of stroke, spinal cord injury, and any other patient groups, which face prolonged bed rest. While this study covers all the available inputs and their combinations, one might have to select a subset of these stimuli depending on the specific patient group. Particularly, for certain patient populations, it can be difficult to collect data for model identification of all the stimuli to cardiovascular variables. Our pilot study investigated the feasibility to find simple models for the best-case scenario, when there are no input restrictions by the target population present, and thus, it leaves studying the group-specific restrictions in this regard for future work.

Various parameters might influence the efficacy of stepping and FES. For stepping, its frequency, the range of motion, and the amount of foot loading can affect the efficacy [45], where the subjects weight bearing affects the foot loading. The FES efficacy can depend on its amplitude, frequency, pulse width, and even electrode placement. In the current work, the pain threshold of healthy subjects limited the applied FES intensities. Application of higher intensities without imposing higher pain might be feasible in some bed-rest patients (e.g., patients with complete paralysis). However, muscle recruitment in such patients is usually limited due to muscle atrophy [15, 34], and therefore, higher FES intensities, do not necessarily result in higher FES efficacy [15, 34, 37].

4.2 Comparison of model structures

The assumptions, in particular about noise and model structures are not necessarily correct, i.e., the human cardiovascular system natural oscillations do not necessarily follow the white noise assumption. Therefore, the comparison of the algorithms solely based on simulation studies might not be reliable, and experimental confirmation can further enhance the reliability of the results. Our simulations showed that for first-order models, the OARX, ARX, and OE structures might similarly perform well. However, statistical analysis of the experimental results revealed that overall, ARX with detrending performs better than OARX.

Therefore, it is recommended that when identification of first-order models is desired, and the ARX structure is considered, the offset be subtracted from the signal before further processing (ARX algorithm) rather than be considered in the optimization of the ARX structure (OARX). This might be explained when we consider that in the ARX structure the noise model is not independent of the system TF and therefore, the inclusion of the offset as another free dimension in the optimization algorithm might worsen the estimation results. For second-order systems, experimental and simulation results are consistent and show that the OE structure performs better than the ARX structure (independent from the way offset is handled). This can be explained by the fact that for second-order models, the overshoot should be differentiated from natural oscillations and this is harder for the ARX structure, as it assumes that the noise model is dependent on the system model, and therefore, the overshoot might be considered as noise and overlooked. For the OE structure, this is less probable as it assumes that the noise structure is independent of the system dynamics, and thus, the overshoot might be recognized better. Therefore, for identification of second-order models, the application of OE rather than ARX is recommended.

Although we acknowledge that the comparison of different model structures (OARX, ARX, and OE) and orders is performed with the assumption that our best-selected model in the identification procedure is the true TF of the system, it should not be ignored that the selected model in comparison with other model structures, orders, etc. is the best model describing the identification set data. Therefore, although the identified models might not be suitable to predict the responses in a new data (e.g., the testing set) due to issues such as nonlinearity, considering them as the true underlying systems to compare different model structures and orders might be a reasonable assumption.

5 Conclusion and outlook

Integration of *K*-fold cross-validation in the identification framework enabled efficient use of data, which is necessary when the goal is modeling physiological responses from human subjects. Only in HR TFs for inclination input, the response could be explained well by a single low-order linear TF and the models were reliable. In all cardiovascular variables, the responses to stepping and change in FES amplitude are dependent on the tilt angle and are highly nonlinear (as confirmed by low prediction performance of the identified models. So, nonlinearities (e.g., through nonlinear transformations) have to be considered for their modeling.

For black-box modeling of the cardiovascular system response to external stimuli, based on the insights provided in Sect. 2.4.7, it is more suitable to use a step input rather than other input types such as PRBS or frequency sweep, particularly when considering low-order models and two-stage identification of a Hammerstein model. When the aim is to identify a first-order model, the OE and ARX structures both perform well. For ARX, it is better to subtract the offset directly rather than considering it as another optimization parameter. For second-order models, OE outperforms the ARX structure.

We could show that responses to stepping and FES are dependent on the tilt angle. Furthermore, the responses are nonlinear. We conclude that exploring these nonlinearities and dependencies is necessary before designing an appropriate controller for early mobilization of bedridden patients.

Acknowledgements We thank Prof. Dr. Kenneth J. Hunt, Bern University of Applied Sciences for his invaluable advice, Francesco Crivelli for fruitful discussions, Maya I. Kamber for the preparation of the ethics documents, as well as Marcello Chiarello and Silvio Nussbaumer for their experimental support. This work was supported by the Commission for Technology and Innovation CTI, Switzerland, and the European Community's Seventh Framework Programme FP7/2007-2013 under Grant Agreement No. 312815-STAMAS

References

1. Adami A, Pizzinelli P, Bringard A, Capelli C, Malacarne M, Lucini D, Simunič B, Pišot R, Ferretti G (2013) Cardiovascular re-adjustments and baroreflex response during clinical reambulation procedure at the end of 35-day bed rest in humans. Appl Physiol Nutr Metab 38(6):673–680
2. Bai EW (2004) Decoupling the linear and nonlinear parts in Hammerstein model identification. Automatica 40(4):671–676
3. Bamford J, Dennis M, Sandercock P, Burn J, Warlow C (1990) The frequency, causes and timing of death within 30 days of a first stroke: the Oxfordshire Community Stroke Project. J Neurol Neurosurg Psychiatry 53(10):824–829
4. Bernhardt P, Mertelmeier T, Hoheisel M (2006) X-ray spectrum optimization of full-field digital mammography: simulation and phantom study. Med Phys 33(11):4337–4349
5. Billings SA (2013) Nonlinear system identification: NARMAX methods in the time, frequency, and spatio-temporal domains. Wiley, Hoboken
6. Bishop CM et al (2006) Pattern recognition and machine learning, vol 1. Springer, New York
7. Bourdin G, Barbier J, Burlem JF, Durante G, Passant S, Vincent B, Badet M, Bayle F, Richard JC, Guérin C (2010) The feasibility of early physical activity in intensive care unit patients: a prospective observational one-center study. Respir Care 55(4):400–407
8. Brower RG (2009) Consequences of bed rest. Crit Care Med 37(10):S422–S428
9. Burtin C, Clerckx B, Robbeets C, Ferdinande P, Langer D, Troosters T, Hermans G, Decramer M, Gosselink R (2009) Early exercise in critically ill patients enhances short-term functional recovery. Crit Care Med 37(9):2499–2505
10. Chi L, Masani K, Miyatani M, Thrasher TA, Johnston KW, Mardimae A, Kessler C, Fisher JA, Popovic MR (2008) Cardiovascular response to functional electrical stimulation and dynamic tilt table therapy to improve orthostatic tolerance. J Electromyogr Kinesiol 18(6):900–907

11. Colombo G, Schreier R, Mayr A, Plewa H, Rupp R (2005) Novel tilt table with integrated robotic stepping mechanism: design principles and clinical application. In: 9th international conference on rehabilitation robotics, 2005. ICORR 2005. IEEE, pp. 227–230
12. Cooper N, Forrest K, Cramp P (2008) Essential guide to acute care. Wiley, Hoboken
13. Cooper R, Fletcher-Shaw TL, Robertson RN et al (1998) Model reference adaptive control of heart rate during wheelchair ergometry. IEEE Trans Control Syst Technol 6(4):507–514
14. Corno M, Giani P, Tanelli M, Savaresi SM (2015) Human-in-the-loop bicycle control via active heart rate regulation. IEEE Trans Control Syst Technol 23(3):1029–1040
15. Craven CTD, Gollee H, Coupaud S, Allan DB (2013) Investigation of robotic-assisted tilt-table therapy for early-stage spinal cord injury rehabilitation. J Rehabil Res Dev 50(3):367–378
16. Cumming TB, Thrift AG, Collier JM, Churilov L, Dewey HM, Donnan GA, Bernhardt J (2011) Very early mobilization after stroke fast-tracks return to walking further results from the phase II avert randomized controlled trial. Stroke 42(1):153–158
17. Czell D, Schreier R, Rupp R, Eberhard S, Colombo G, Dietz V (2004) Influence of passive leg movements on blood circulation on the tilt table in healthy adults. J Neuroeng Rehabil 1(1):4
18. Dittmer D, Teasell R (1993) Complications of immobilization and bed rest. part 1: musculoskeletal and cardiovascular complications. Can Fam Physician 39:1428
19. Fortney SM, Schneider VS, Greenleaf JE (1996) The physiology of bed rest. In: Comprehensive physiology, Wiley. doi:10.1002/cphy.cp040239
20. Graham GM, Thrasher TA, Popovic MR (2006) The effect of random modulation of functional electrical stimulation parameters on muscle fatigue. IEEE Trans Neural Syst Rehabil Eng 14(1):38
21. Hahn JO, Dumont G, Ansermino JM et al (2012) System identification and closed-loop control of end-tidal co in mechanically ventilated patients. IEEE Trans Inf Technol Biomed 16(6):1176–1184
22. Hainsworth R, Al-Shamma Y (1988) Cardiovascular responses to upright tilting in healthy subjects. Clin Sci 74(Pt 1):17–22
23. Hunt K, Allan D (2009) A stochastic Hammerstein model for control of oxygen uptake during robotics-assisted gait. Int J Adapt Control Signal Process 23(5):472–484
24. Hunt KJ, Munih M, Donaldson Nd, Barr F et al (1998) Investigation of the Hammerstein hypothesis in the modeling of electrically stimulated muscle. IEEE Trans Biomed Eng 45(8):998–1009
25. Lee DS, Lemieux T (2009) Regression discontinuity designs in economics. Tech. rep, National Bureau of Economic Research
26. Leontaritis I, Billings S (1987) Experimental design and identifiability for non-linear systems. Int J Syst Sci 18(1):189–202
27. Ljung L (1998) System identification. Springer, Berlin
28. Luther MS, Krewer C, Müller F, Koenig E (2008) Comparison of orthostatic reactions of patients still unconscious within the first three months of brain injury on a tilt table with and without integrated stepping. a prospective, randomized crossover pilot trial. Clin Rehabil 22(12):1034–1041
29. Matalon SV, Farhi LE (1979) Cardiopulmonary readjustments in passive tilt. J Appl Physiol 47(3):503–507
30. Menard S (2000) Coefficients of determination for multiple logistic regression analysis. Am Stat 54(1):17–24
31. Morris PE (2007) Moving our critically ill patients: mobility barriers and benefits. Crit Care Clin 23(1):1–20
32. Narendra KS, Annaswamy AM (1987) Persistent excitation in adaptive systems. Int J Control 45(1):127–160
33. Parati G, Saul JP, Di Rienzo M, Mancia G (1995) Spectral analysis of blood pressure and heart rate variability in evaluating cardiovascular regulation a critical appraisal. Hypertension 25(6):1276–1286
34. Riener R, Fuhr T (1998) Patient-driven control of FES-supported standing up: a simulation study. IEEE Trans Rehabil Eng 6(2):113–124
35. Sarabadani A, Bernasconi S, Klamroth-Marganska V, Nussbaumer S, Riener R (2013) Model-free predictive control of human heart rate and blood pressure. In: IEEE 13th international conference on bioinformatics and bioengineering (BIBE). IEEE, pp 1–5
36. Sarabadani Tafreshi A, Klamroth-Marganska V, Nussbaumer S, Riener R (2015) Real-time closed-loop control of human heart rate and blood pressure. IEEE Trans Biomed Eng 62(5):1434–1442
37. Sarabadani Tafreshi A, Riener R, Klamroth-Marganska V (2016) Distinctive steady-state heart rate and blood pressure responses to passive robotic leg exercise and functional electrical stimulation during head-up tilt. Front Physiol 7:612
38. Schwartz CE, Stewart JM (2012) The arterial baroreflex resets with orthostasis. Front Physiol 3:461. doi:10.3389/fphys.2012.00461
39. Siegel S (1956) Nonparametric statistics for the behavioral sciences. McGraw-Hill, New York, US, p 312. http://lib.ugent.be/catalog/rug01:000005357
40. Smith JJ, Porth CM, Erickson M (1994) Hemodynamic response to the upright posture. J Clin Pharmacol 34(5):375–386
41. Smith JO (2007) Introduction to digital filters: with audio applications, vol 2. W3K Publishing. http://www.w3k.org/books/
42. Su SW, Huang S, Wang L, Celler BG, Savkin AV, Guo Y, Cheng TM (2010) Optimizing heart rate regulation for safe exercise. Ann Biomed Eng 38(3):758–768
43. Su SW, Wang L, Celler BG, Savkin AV, Guo Y (2007) Identification and control for heart rate regulation during treadmill exercise. IEEE Trans Biomed Eng 54(7):1238–1246
44. Toska K, Walløe L (2002) Dynamic time course of hemodynamic responses after passive head-up tilt and tilt back to supine position. J Appl Physiol 92(4):1671–1676
45. Wieser M, Gisler S, Sarabadani A, Ruest RM, Buetler L, Vallery H, Klamroth-Marganska V, Hund-Georgiadis M, Felder M, Schoenberger JL et al (2014) Cardiovascular control and stabilization via inclination and mobilization during bed rest. Med Biol Eng Comput 52(1):53–64
46. Wieser M, Haefeli J, Bütler L, Jäncke L, Riener R, Koeneke S (2010) Temporal and spatial patterns of cortical activation during assisted lower limb movement. Exp Brain Res 203(1):181–191
47. Yoshida T, Masani K, Sayenko DG, Miyatani M, Fisher JA, Popovic MR (2013) Cardiovascular response of individuals with spinal cord injury to dynamic functional electrical stimulation under orthostatic stress. IEEE Trans Neural Syst Rehabil Eng 21(1):37–46

Amirehsan Sarabadani Tafreshi received the M.Sc. degree in robotics, systems and control, in 2011, from ETH Zurich, Zurich, Switzerland, where he is currently working toward the Ph.D. degree at Sensory-Motor Systems Lab. His research interests include rehabilitation robotics, human–robot interaction, pattern recognition, and biomedical signal processing.

Jan Okle received the M.Sc. in robotics, systems and control, in 2016, from ETH Zurich, Zurich, Switzerland. During his master studies, he participated in an exchange program with Massachusetts Institute of Technology (MIT) and did an internship at Verity Studios, a start-up company of ETH Zurich that develops drones.

Verena Klamroth-Marganska studied human medicine at Freie Universität and Humboldt-Universität, Berlin, Germany, and received the Doctoral degree from WestfälischeWilhelms-Universität Münster, Münster, Germany, in 2004. From 2000 to 2006, she was a Research Assistant with the Institute of Human Genetics at University Hospital Münster, Germany, and from 2006 to 2007, was an Intern at the Department of Neurology, MEDIAN KLINIK, Berlin, Germany. Since 2008, she has been a Senior Research Associate at the Sensory-Motor Systems Lab, Department of Health Science and Technologies, ETH Zurich, Zurich, Switzerland.

Robert Riener studied mechanical engineering from TU München, München, Germany, and from the University of Maryland, College Park, MD, USA. He received the Dr. Ing. degree in engineering from the TU München in 1997. After postdoctoral work from 1998 to 1999 at the Centro di Bioingegneria, Politecnico di Milano, he returned to TU Munchen, where he completed his Habilitation in the field of Biomechatronics in 2003. In 2003, he became an assistant professor at ETH Zurich, Zurich, Switzerland, and Spinal Cord Injury Center of the University Hospital Balgrist ("double-professorship"). Since 2010, he has been a full Professor for Sensory-Motor Systems, ETH Zurich. Since 2012, he has been with the Department of Health Sciences and Technology and since 2016, he is the head of this Department. Riener has published more than 400 peer-reviewed journal and conference articles, 20 books and book chapters and filed 20 patents. He has received 18 personal distinctions and awards including the Swiss Technology Award in 2006, the IEEE TNSRE Best Paper Award 2010, and the euRobotics Technology Transfer Awards 2011 and 2012. Riener's research focuses on the investigation of the sensory-motor interactions between humans and machines. This includes the development of user-cooperative robotic devices and virtual reality technologies applied to neurorehabilitation. Riener is the initiator and organizer of the Cybathlon 2016.